CHAPTER 62

Spatial variation of wave group statistics and representative wave-heights of swell

Akiyuki UKAI, Takashi YASUDA, Kazunori ITO

Abstract

This study derives a practical equation that can describe the weakly nonlinear waves having an arbitrary spectral form and propagating unidirectionally from deep to shallow water, and carries out the numerical simulation using the equation. Based on the simulated results, some investigations are made on the characteristics of spatial variation of wave group and representative wave-heights in the propagation process.

1. Introduction

Characteristics of grouped waves propagating from deep to shallow water are clearly important for engineering purpose, but are little made clear because the difficulty of the observation of in field. Regretably, most of usual investigations are concerned with the statistics of wave grouping derived from temporal wave registrations obtained at fixed locations and lack a view point that the statistics may change spatially during the propagation of the grouped waves. Hence, in order to investigate on the spatial variations of the characteristics during the propagation from deep to shallow water, it is essentially required to develop a tractable equation that can be easily solved for the nonlinear waves having an arbitrary spectral bandwidth and propagating from deep to shallow water and employ a theoretical approach using the equation, instead of the approach based on the field observation.

 ^{*} Eng., Civil Eng. Dept., Penta-Ocean Construction Co., Ltd., Koraku 2-Chome, Bunkyo-ku, Tokyo 112, JAPAN

^{**} Prof., Dept. of Civil Eng., Gifu Univ., Gifu 501-11, JAPAN

^{***}Graduate student, ditto

In this study, we suggest a single tractable equation of spatial evolution type for describing the unidirectional propagation of swell and carry out numerical simulations using the equation. Further, based on the simulated results, we investigate intensively on the characteristics of spatial variations of wave group statistics and representative wave-heights in the propagation process.

2. A model equation for swell 2.1 Derivation

we derive a tractable equation that can easily describe weakly nonlinear waves having an arbitrary spectrum and propagating unidirectionally from moderately deep to shallow water, by modifying the dispersion term of the following perturbed KdV equation so as to give the correct linear dispersion relation of surface gravity waves.

$$\eta_x + \frac{1}{\sqrt{gh}}\eta_t + \frac{3}{2}\frac{1}{h\sqrt{gh}}\eta_{t} + \frac{1}{6}\frac{h^2}{(gh)^{3/2}}\eta_{tt} + \frac{1}{4}\frac{h_x}{h}\eta = 0$$
(1)

where the subscripts x and t denote partial differentiations with regard to them, x the horizontal coordinate, t the time, η the temporal water surface elavation, h the mean water depth in the propagation process and g the accelation of gravity.

To our best knowledge, there is no equation of spatial evolution type such that can describe actually the propagation process of weakly nonlinear waves having arbitrary spectrum. The necessary conditions for the equation are as follows:

i) Only if the temporal water surface elevation at any fixed location is given as a boundary condition, the equation can describe its spatial evolution over a sloping bottom from deep to shallow water.

ii) The equation can be applied to the swell having an arbitrary spectrum.

iii) The equation should be tractable so as to be for numerical simulation of the long distance propagation.

An equation of wave motion of spatial evolution type can be written for linear waves having correct dispersion relation and propagating on the moving coordinate with the speed of \sqrt{gh} as

$$\partial_x \eta + \int_{-\infty}^{\infty} F(\tau - \sigma) \partial_\sigma \eta \, d\sigma = 0$$
 , (2)

$$F(\tau - \sigma) = \frac{1}{2\pi} \int_{-\infty}^{\infty} \frac{c(\omega) - \sqrt{gh}}{c(\omega)} e^{-i\omega(\tau - \sigma)} d\omega$$

$$\tau = \int dx / \sqrt{gh} - t, \quad \omega = 2\pi f \qquad , \qquad (3)$$

where

and $c(\omega)$ is the wave speed of linear dispersive waves. Here, assuming its solution as

$$\eta = \sum_{-\infty}^{\infty} A_m(x) \exp\left(i\omega_m \tau\right) \quad , \tag{4}$$

and treating this equation on the frequency domain, we obtain the following mode rate equation.

$$\frac{dA_m}{dx} + ik(\omega_m)[C(\omega)/\sqrt{gh} - 1]A_m = 0, \qquad (5)$$

Further, introducing the nonlinear term $3/2\eta\eta_1$ and the shoaling term $h_x\eta/4$ included in the perturbed KdV equation shown in eq(1), we obtain a single tractable equation of spatial evolution type and call it as a model equation for swell unidirectionally propagating from moderately deep to shallow water.

$$d\tilde{A}_{m}/dx^{*} + ik_{m}^{*}(c^{*}-h^{*1/2})\tilde{A}_{m} + \sum_{j=-\infty}^{\infty} i\frac{3}{2}k_{m}^{*}h^{*-7/4}\tilde{A}_{m-j}\tilde{A}_{j} = 0 , \qquad (6)$$

$$m: -\infty \sim \infty$$

$$x^{*} = x/h_{0}, \quad k_{m}^{*} = k(\omega_{m})h_{0}, \quad h^{*} = h/h_{0}, \\ c^{*} = c(\omega_{m})/\sqrt{gh_{0}}, \quad A_{m}/h_{0} = \tilde{A}_{m}h^{*-1/4}, \quad \}$$
(7)

This equation has two conserved quantities of 1st and 2nd order are derived from the model equation as

$$\frac{d}{dx}I_{1} = -\frac{3}{4} \frac{\eta^{2}}{\sqrt{gh^{3}}} \Big|_{0}^{T_{0}} - \int_{0}^{T_{0}} L[\eta] dt, \quad I_{1} = \int_{0}^{T_{0}} \eta dt \quad , \tag{8}$$

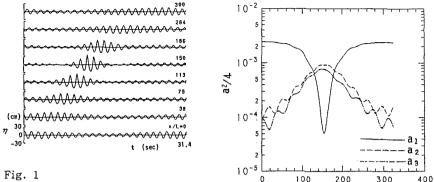
$$\frac{d}{dx}I_2 = -\frac{\eta^3}{2\sqrt{gh^3}} \Big|_0^{T_0} - \int_0^{T_0} \eta L[\eta] dt, \quad I_2 = \int_0^{T_0} \frac{\eta^2}{2} dt \quad , \tag{9}$$

where

$$L[\eta] = \sum_{m=-\infty}^{\infty} i \left[\sqrt{(k_m/h) \tanh k_m h} - k_m \right] A_m e^{i\omega_m t} , \qquad (10)$$

Assuming the periodicty of η with an observation period T₀ on time domain, we can put the right hand sides of eqs(8) and (9) zero, because of the relation $A_m = A_{-m}$ and the fact that $\omega(k_m)$ is the odd function of k_m . Thus, we can evaluate the accuracy of the numerical solution by examining the conservativeness of I₁ and I₂. Here, the equation was solved under the accuracy that the errors for both the conservation laws are kept within 0.1 %.

Furthermore, it should be emphasized that the modulational instability occurs in the wave train governed by the model equation, although the nonlinear term of the equation is identical with that of the KdV



Wave train of a quasi-monochromatic

wave train.

Fig. 2 Modulation of peak and its side band modes.

×/L

equation which cannot express the instability. Figure 1 shows the spatial evolution of a quasi-monochromatic wave train governed by the model equation. Figure 2 shows the modulation of the peak mode and its sideband modes and explains clearly that the modulation and demodulation successively occur.

2.2 Accuracy

Since the model equation is not derived consistently from the fundamental equation of hydrodynamics, we are required to examine the applicability before carrying out the numerical simulations of long distance propagation of swell through the model equation.

At first, we examined the accuracy of the model equation by comparing with the exact Stokes waves. Figure 3 [Yasuda et al., 1989] shows the applicable region of the model equation and the KdV equation. The boundaries in this figure indicate the critical values of ka and kh under which the maximum value of the error E_1 , defined by

$$E_1(t) = \int_{-\pi/k}^{\pi/k} [\gamma(x,t) - Y(x-ct)]^2 dx \Big/ \int_{-\pi/k}^{\pi/k} Y^2 dx , \qquad (11)$$

is kept within 0.06. Here, η denotes the numerical solution of the model equation, Y the exact Stokes wave solution and c is phase speed. Hence, E₁ can be used as an error criterion indicating the accuracy of the numerical solution to the exact solution of steady wave. It could be said that the model equation is applicable within the boundaries shown in figure 3 and that the model equation is superior to the KdV equation in the range of kh>0.8. However, the model equation does not unexpectedly work so well for the waves in

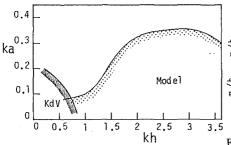


Fig. 3

Applicable region derived from the comparisons with the exact Stokes wave.

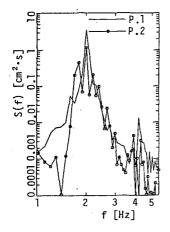


Fig. 5 Power spectra measured at P.1 and P.2

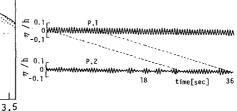


Fig. 4

Temporal water surface elevations measured at P.1, and P.2

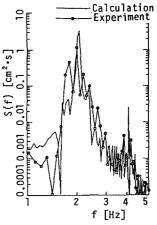


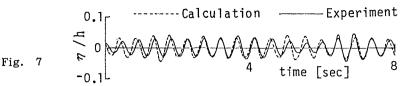
Fig. 6

Comparison of power spectra at P.2 between the experimental result and the caliculated one.

deeper water than kh>3.3, because its nonlinear term is valid only for long waves with kh<<1.

Secondly, we examined experimentally the applicability of the model equation to the quasi-monochromatic waves suffering from the modulational instability. Figure 4 shows the temporal water surface elevations at P.1 and P.2 of a modulational wave train generated in a wave flume [1mx1mx54m] having a servo-controlled wave maker . The distance between the measuring location P.1 and P.2 is $kx=42\pi$ in this case. It is conjectured from Fig. 5 that the modulation observed at P.2 is primality due to the growth of the side-band modes of the spectral peak .

Figure 6 shows the comparison of power spectra at P.2 between the measured result and the simulated one.



Comparison of water surface profile at P.2 between the experimental result and the simulated one.

Figure 7 indicates the comparison of temporal wave profile at P.2 between both the results. The simulation carried out by making the waves measured at P.1 propagate to P.2 through the model equation. Both the results corresponds to each other in rough trend. However, it should be noticed that the modulation of the simulated waves is considerably weak and the side-band modes of the simulated waves are not so strengthened in comparison with those of the measured waves. Hence, it should be noted that the growth of the modulation is evaluated a little weakly as far as the model equation is used.

Finally, we examined the applicability of the model equation to irregular waves having various spectral bandwidth, by generating the desired waves of which initial spectra are the Wallops type in the aforementioned wave flume and comparing the measured wave profiles at P.2 with the results simulated as well as the case of the quasi-monochromatic waves mentioned above. The error criterion E_2 for evaluating the applicability of the model equation to the irregular waves is defined as

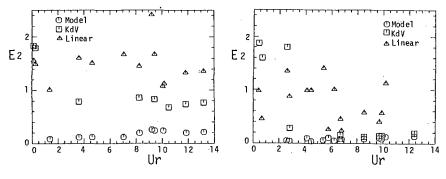
$$E_{2}(x) = \int_{0}^{T_{0}} (\eta_{\rm ob} - \eta_{\rm cal})^{2} dt / \int_{0}^{T_{0}} \eta_{\rm ob}^{2} dt \quad , \qquad (12)$$

This denotes the difference with the water surface elevation including the propagation speed between the simulated result $\eta_{q,q,1}$ and the measured one $\eta_{q,b}$ at P.2. The relation between the error criterion E_2 and the Ursell number(Ur) is shown in Fig. 8. Qp in the figure denotes the spectral peakedness parameter.

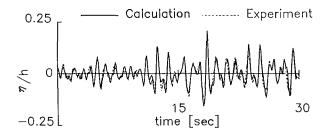
Figure 9 shows the comparison of temporal wave profile at P.2 between the measured result and the simulated one in the case that the aformentioned erroe E_2 is 0.23.

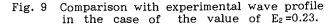
3 Propagation of swell

Numerical simulations using the model equation are made in order to investigate on the characteristics of spatial variations of wave grouping, by giving the following temporal water surface elevation with the desired statistics to the model equation as the



(a) $Qp\simeq 2$ (b) $Qp\geq 4$ Fig. 8 The relation between error criterion E_2 and Ur.





boundary condition at origin.

$$\eta(0,\tau) = \sum_{n=0}^{\infty} 2|A_n| \sin\left(2\pi f_n \tau + \varepsilon_n\right) \quad , \tag{13}$$

where, ε_n is the random phase angle distributed uniformly between 0 and 2π , M the number of the Fourier modes and 2^{11} in this study, A_n denotes the amplitude of the nth Fourier mode and is related to the spectral density S(f) as

$$A_j = \sqrt{2 \int_0^\infty S(f) \delta(f - f_j) df/T_0} \quad , \tag{14}$$

The initial spectrum S(f) is given so as to have the Wallops type and the values of parameters governing the spectral form are determined for the initial waves so as to have the desired statistics with the dispersion parameter kh, the nonlinear parameter ka and the spectral bandwidth parameter m. Here, k is the wave number which is correspondent to the frequency at the spectral peak and is calculated through the

111	5	15	30	55
Q_p	2.00	4.04	5.90	8.07

Tablu 1 The relation between m and Qp.



Wave profile of numericaly simulated waves during the propagation (kh=2.0, ka=0.15 and m=15).

linear dispersion relation, and the amplitude a equals to the half of the significant wave-height $H_1/_3$. The value of m is about 5 in the case of wind waves and is over 15 for swell. Table 1 indicates the present relation between m and Qp.

Figure 10 shows the temporal water surface elevations at x/L=0, 33 and 146 of the waves simulated with using the model equation under the initial statistics of kh=2.5, ka=0.15 and m=15.

4 Spatial variation of wave grouping

Groupiness Factor(GF) defined by Funke and Mansard[1979] is employed here as statistics of describing wave grouping and its spatial variation dependent on the initial values is investigated for the simulated waves. Figure 11 indicates the spectral forms

103 103 103 TTIM x/L=0 33 146 10² 102 102 S (m²sec) 101 101 101 1 1 1 1 1 1 1 1 1 100 100 100 10-1 10-1 10-1 0.01 0.1 1 0.01 0.1 1 0.01 0.1 f (Hz)

Fig. 11

Variation of the spectral form of the wave shown in Fig.10.

of nonlinear waves shown in Fig. 10. The remarkable growth of the modulation at x/L=33 is supposed to be due to the pronounciation of side-band modal components.

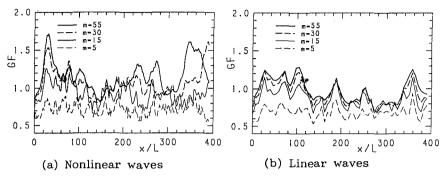


Fig. 12

Influences of bandwidth parameter m on the spatial variation of GF of nonlinear and linear waves. (kh=2.5, ka=0.15)

Figure 12(a) shows the spatial variation of GF of the waves simulated with the model equation under the initial statistics of kh=2.5,ka=0.15 and some spectral bands of m=5,15,30 and 55. The spatial variations of GF of linear waves under the same initial statistics are 12(b), in order to show the influence of in Fig. nonlinearity on wave grouping. It is found from the figures that not only the value of GF of nonlinear waves but also that of linear waves varies spatially the propagation. The former variation is during conjectured be caused by the modulational to clearly due to instability, while the latter one is linear combination of the Fourier modes. However, the former variation gets to exceed greatly the latter one and the influence of the nonlinearity becomes dominant as the value of m increases, that is, the spectral bandwidth becomes narrower.

The influence of kh on the spatial variations of GF is examined. Figure 13 shows the influence under the initial statistics of ka=0.12,m=5 and 30 and kh=1.04, 1.72 and 3.11. In the broad band case of m=5, the spatial variation of GF is not so dependent on the value of kh and the influence of kh is not so conspicuous. However, under the narrow band spectrum of m=30, the difference between the case of kh=1.04 and those of kh=1.72 and 3.11 is very large. This remarks that wave grouping catastrophically changes at the vicinity of kh=1.40, which is the critical point of the modulational instability in the model equation, under the spectrum of finite bandwidth.

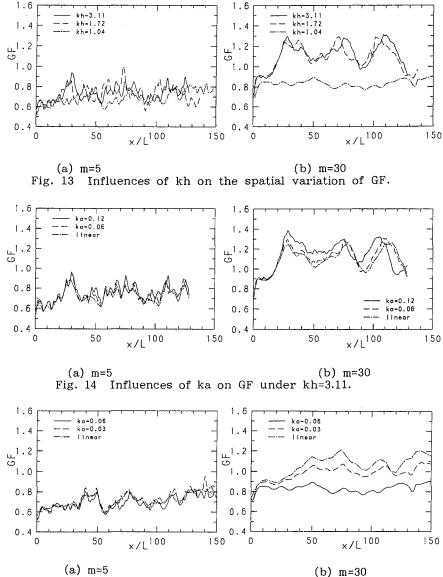


Fig. 15 Influences of ka on GF under kh=1.04.

In oder to investigate the nonlinear effect on the variation of GF, we carried out some numerical simulations. Figures 14 and 15 show the influence of the value of ka on the variation of GF. The statistics of initial waves are kh=3.11, ka=0.06 and 0.12, m=5 and 30 in the Fig. 14. And, those of initial waves in Fig.

15 are kh=1.04, ka=0.03 and 0.06, m=5 and 30. In these cases, the growth of wave grouping becomes strengthened as the spectral bandwidth get to be narrower from m=5 to m=30. These results show that the effect of nonlinearity on the growth of wave grouping could be almost ignored so long as the value of ka is less than 0.12.

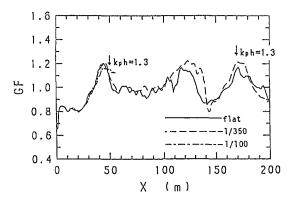


Fig. 16

Influences of bottom slope on the spatial evolution of GF

In order to investigate the effect of bottom slope on the variation of GF, we carried out the numerical simulation for three different values of bottom slope. The statistics of the initial waves kh=3.11, are ka=0.06 and m=15, and the simulation results are shown in Fig.16. It is found that the bottom slope has influence on the behavior of GF so long as the little value of kh is larger than 1.3. From this result, we conclude that can the spatial variation of wave grouping should be considered as a result of the modulational instability rather than that of shoaling wave.

6. Spatial variations of representative wave-heights

If wave grouping is a consequence of finely tuned focussing of linear wave trains or modulational instability of nonlinear wave trains , it is natural the influence of wave grouping comes not only that to a time sequence of zero-cross waves but also to representative wave-heights. Figure 17 shows spatial variations of representative wave-heights of the swell of which initial statistics are kh=2.5, ka=0.15, m=5 and 30. Since the swell propagate on a flat bottom , the values of η_{rms} , \overline{H} and $H_{1/3}$ are almost invariant as the matter of course. On the other hand, the value of $H_{m,a,x}$ varies greatly in the propagation process and the

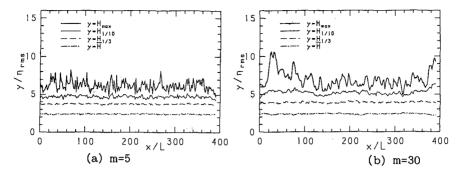


Fig. 17 Spatial evolution of representative wave-heights.

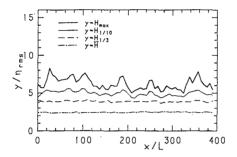


Fig. 18

Spatial evolution of representative wave-heights in linear wave field

ratio of $H_{m,a,x}/H_{1/3}$ often exceeds 2.0 that is the value employed in the design of offshore structures. Figure 18 shows spatial variations of representative waveheights of the liner wave under the initial statistics of kh=2.5,ka=0.15 and m=30. The value of $\overline{H},\ H_{1\times3}$ and $H_{1,10}$ are similar to those shown in Fig.17(b). The value of $H_{m,a,x}$ varies in the prppagation process, but the ratio of $H_{m,a,x}/H_{1/3}$ never exced 2 in this linear calculation. Therefore the appearance of a region with $H_{n,s,x}/H_{1/3}>2$ which was observed in Fig. 18 can be ascribed to the nonlinear interaction. Figure 19 shows the relation between GF and H_{max} under the initial statistics of kh=2.5,ka=0.15 and m=30. The variation of GF agrees well with that of $H_{m,a,x}$. This indicates that the variation of $H_{m,e,\chi}$ is dependent on GF in the propagation process. Figure 20 shows the relative frequency of the ratio H_{max}/\overline{H} derived from the surface elevation at each location in the propagation process. A solid line denotes the relative frequency of the waves of which zero-cross wave-heights obey the Rayleigh distribution. Although there is no significant

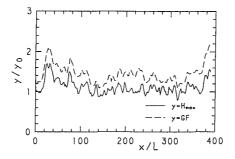


Fig. 19 the present relation betweek GF and $H_{m\mbox{ ax}}$

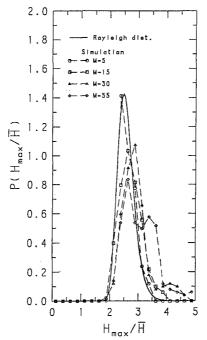


Fig. 20 Relative frequencies of the ratio $H_{m ax}/\overline{H}$ at each location in the propagation process.

difference in the case of m=5 between the result simulated by the model equation and that based on the Rayleighan, the difference between both the results becomes significant in the case of m=30. This demonstrates that the consideration of the influence of wave grouping becomes necessary in the reliable prediction of design waves as the spectral band-width gets to narrower.

7. Conclusions

The accuracy and applicable region of the model equation was made clear with respect to the wave statistics of kh and ka or Ur through experimental examinations. Wave groups seen in the swell having kh ≥ 0.14 , ka ≥ 0.12 and m ≥ 30 are originated primarily by the modulational instability, although the other wave groups are generally consequences of linear combination of different, independent Fourier modes. Wave packets exhibited generally in the swell varies spatially during the propagation differently from the envelope solitons and should be treated as unsteady phenomena. The characteristics of their spatial variations were made clear through GF and representative wave-heights and were found to be dependent on the statistics of kh, ka and m. The maximum wave-height Hmex is closely reated with the wave grouping and the relative frequency of the ratio H_{max}/\overline{H} considerably deviates from that based on the Rayleigh distribution under the narrow band spect-rum of m≥30.

The authors wish to express their thanks to Dr.M.Tanaka for his valuable advices.

Referrences

Yasuda,T.,M.Tanaka,A.Ukai and Y.Tsuchiya(1988) Proc. of Coastal Eng., Vol. 35, JSCE pp.93-97. Yasuda,T.,M.Tanaka,K.Ito (1989) Proc. of Coastal Eng., Vol. 36, JSCE pp.104-108. Funke,E. and E.Mansard(1979) Hyd. Lab. Rep. LTR-HY-66, NRC Canada, 54p.